

Coking resistance of Pt–Sn alloys probed by acetylene chemisorption

Chameli Panja, Najat A. Saliba and Bruce E. Koel *

Department of Chemistry, University of Southern California, Los Angeles, CA 90089-0482, USA

Received 20 April 2000; accepted 1 June 2000

Acetylene (C_2H_2) is a reactive molecule with a low C:H stoichiometry that can be used to evaluate aspects of the resistance of metal-based catalysts to the formation of carbonaceous residue (coking). Herein we summarize our results for C_2H_2 chemisorption and thermal reaction on four well-defined, ordered surface alloys of Pt–Sn prepared by Sn vapor deposition on Pt(100) and Pt(111) single crystals under UHV conditions. While chemisorption of C_2H_2 under UHV conditions on Pt is completely irreversible, i.e., thermal decomposition leads to complete conversion of the chemisorbed monolayer into surface carbon, alloying with Sn strongly reduces the amount of carbon thus formed. In addition, the temperature for complete dehydrogenation of the carbonaceous residue formed from acetylene decomposition (polymerization) is increased by up to 100 K, from 760 to 860 K. Both of these phenomena are consistent with observations of increased lifetimes and decreased coking for technical Pt–Sn bimetallic catalysts compared to Pt catalysts used for hydrocarbon conversion reactions.

Keywords: acetylene, catalysts, coking, chemisorption, alloys, Pt–Sn, carbon, hydrocarbons

1. Introduction

Alumina-supported Pt–Sn catalysts have been the subject of many basic studies because of the importance of these catalysts in refining and petroleum chemistry, particularly in reforming reactions [1–3]. While there is strong data indicating that Pt–Sn alloy phases are not formed on the active reforming catalysts using Al_2O_3 supports [4,5], the complexity of the materials systems causes difficulties in unambiguously establishing the activity and identity of all the phases present on the catalyst under working conditions. Indeed, Pt–Sn alloy formation has been given as an important contributor to improved reforming selectivity and activity maintenance [6–8]. Furthermore, there are useful catalysts that have been reported to have good performance for a variety of reactions where Pt–Sn alloy phases are fairly clearly identified as the metallic phase responsible for the observed chemistry [9,10]. Thus it is useful to probe further the influence of alloyed Sn on inhibiting carbon build-up on Pt surfaces in order to better understand the origin of decreased coking for these bimetallic catalysts.

C_2H_2 is a reactive molecule with a low H:C stoichiometry: a suitable “coke precursor”. Adsorption of acetylene on a variety of low-index Pt surfaces has been studied previously [11–17]. On Pt(100) [11] and Pt(111) [13–18] complete thermal decomposition to surface carbon and $H_{2(g)}$ occurs under UHV conditions. We found previously that decomposition of acetylene on Pt(111) was reduced by alloying the surface with Sn, reducing carbon formation on the surface by promoting reversible acetylene adsorption and C–C bond coupling reactions leading to de-

sorption of butadiene and benzene [18]. Still, about 35% of the adsorbed acetylene monolayer decomposed on the $(\sqrt{3} \times \sqrt{3})R30^\circ$ -Sn/Pt(111) alloy with $\theta_{Sn} = 0.33$. About 10% of the adsorbed acetylene underwent cyclization to form benzene [18].

Two alloys can also be formed by vapor deposition of Sn on the Pt(100) surface, and the structure and composition of these two alloys are different from those on Pt(111) [19–22]. We report here several results of a more extensive investigation [23] of the adsorption and reaction of acetylene on two ordered Sn/Pt(100) alloyed surfaces. We compare these results to those on Sn/Pt(111) alloy surfaces in order to further elucidate effects of alloyed Sn on inhibiting carbon deposition on Pt surfaces.

2. Experimental

All of the experiments were performed in a stainless UHV chamber described elsewhere [24], which had a base pressure of 8×10^{-11} Torr and was equipped with a four-grid low-energy electron diffraction (LEED) optics, double-pass cylindrical mirror analyzer (CMA) for Auger electron spectroscopy (AES), ion sputtering gun, UTI-100C quadrupole mass spectrometer (QMS) for temperature-programmed desorption (TPD), and various metal and gas dosing facilities.

The Pt(100) crystal was cleaned by repeated cycles of Ar^+ ion sputtering and oxidation at 1200 K with $P_{O_2} = 5 \times 10^{-7}$ Torr. The surface purity and order were checked by AES and LEED. The crystal could be resistively heated to 1200 K and cooled by using liquid nitrogen to 95 K. The temperature was measured by a chromel–alumel ther-

* To whom correspondence should be addressed.

mocouple spot-welded to the side of the crystal. All of the TPD experiments were done utilizing a linear heating rate of 4 K/s. d_2 -acetylene (C_2D_2) (Cambridge Isotope Laboratories, 99% purity) was used as received and dosed onto the crystal through a Varian[®] leak valve connected to a multichannel array gas doser positioned directly in front of the crystal surface.

Two ordered surface alloys can be formed on Pt(111) following Sn deposition and annealing, as previously reported [19,20]. These are denoted as the (2×2) and the $(\sqrt{3} \times \sqrt{3})R30^\circ$ -Sn/Pt(111) surface alloys with $\theta_{Sn} = 0.25$ and 0.33 ML, respectively. On Pt(100), two different alloyed surfaces can be formed by a similar procedure. These two alloys are denoted as the $c(2 \times 2)$ and the $(3\sqrt{2} \times \sqrt{2})R45^\circ$ -Sn/Pt(100) surface alloys with $\theta_{Sn} = 0.50$ and 0.67, respectively [21,22]. All of these surface alloys are quite “flat”, with an outward buckling distance for Sn (above the Pt surface plane) of ~ 0.20 Å. The $c(2 \times 2)$ surface alloy has a “checker board” geometric structure, with one-half of the lattice positions each occupied by Sn and Pt and where each surface Pt atom has only Sn nearest neighbors and *vice versa* [21]. Low energy alkali ion scattering spectroscopy (ALISS) suggested that the $(3\sqrt{2} \times \sqrt{2})R45^\circ$ -Sn/Pt(100) surface alloy had a geometric structure similar to that of the $c(2 \times 2)$ alloy, and was composed of small $c(2 \times 2)$ alloy domains with the same buckling distance within the domains [22]. At this time, the $(3\sqrt{2} \times \sqrt{2})R45^\circ$ -Sn/Pt(100) alloy structure has not been fully determined. STM studies in our lab are underway to further probe the $(3\sqrt{2} \times \sqrt{2})R45^\circ$ -Sn/Pt(100) alloy and the relationship that it has to the structure of the bulk $Pt_3Sn(100)$ surface. For brevity in the rest of this paper, the (2×2) -Sn/Pt(111) and the $(\sqrt{3} \times \sqrt{3})R30^\circ$ -Sn/Pt(111) surface alloys will be referred to as the (2×2) and the $\sqrt{3}$ alloys and the $c(2 \times 2)$ -Sn/Pt(100) and the $(3\sqrt{2} \times \sqrt{2})R45^\circ$ -Sn/Pt(100) alloys will be referred to as the $c(2 \times 2)$ and the $3\sqrt{2}$ alloys, respectively.

Acetylene, benzene, and butadiene TPD curves on both Sn/Pt(111) and Sn/Pt(100) surface alloys were normalized using the results reported previously for Sn/Pt(111) and coverage calibrations on Sn/Pt(100) using XPS and TPD, as reported elsewhere [23].

3. Results and discussion

Thermal desorption spectra of molecular acetylene in TPD following acetylene exposure on Pt and Sn/Pt surface alloys are compared in figure 1. On clean hex-Pt(100) [23], irreversible adsorption of C_2D_2 occurs; D_2 and a small amount of ethylene (C_2D_4) desorb from the surface, and carbon is left on the surface. This is consistent with previous studies [11]. XPS can be used to quantify the extent of irreversible adsorption, and we find that about 90% of the chemisorbed acetylene monolayer undergoes decomposition on Pt(100) [23].

The amount of C_2H_2 desorption from the chemisorbed acetylene monolayer is increased by alloying Sn into the

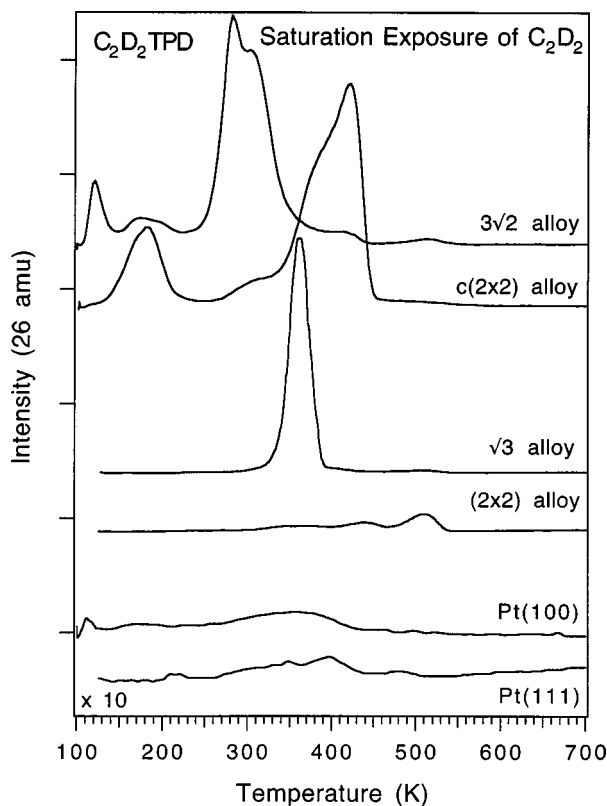


Figure 1. d_2 -acetylene (C_2D_2) TPD curves after saturation d_2 -acetylene exposures on Pt and Pt–Sn alloys at 100 K.

Pt(100) surface. This phenomenon was predictable based on our previous studies of Sn/Pt(111) surface alloys [18]. Only 2% of an acetylene monolayer desorbed molecularly from clean Pt(111), but increasing amounts of Sn in the (2×2) and $\sqrt{3}$ alloys increased the molecular desorption of acetylene.

Acetylene is more weakly chemisorbed on Pt–Sn alloys than on Pt surfaces. In both sets of Sn/Pt(111) and Sn/Pt(100) surface alloys, a higher Sn concentration shifted the desorption temperature of acetylene to lower temperatures. However, C_2D_2 is apparently more strongly bound on the $c(2 \times 2)$ -Sn/Pt(100) alloy with $\theta_{Sn} = 0.5$ ML than on the (2×2) -Sn/Pt(111) surface with $\theta_{Sn} = 0.33$ ML (if C_2D_2 desorption is rate limiting).

Figure 2 shows the D_2 evolution in TPD after saturation doses of d_2 -acetylene on several surfaces. Measurements of D_2 TPD peak areas were used to quantify the amount of acetylene decomposition that occurs during TPD. Only 72% of the amount of acetylene decomposition on Pt(111) occurs on the (2×2) alloy, and only 35% of that on Pt(111) decomposes on the $\sqrt{3}$ alloy. This effect for the Sn/Pt(100) alloys is larger with higher Sn concentration, i.e., the decomposition of acetylene is decreased to only 7% of that on Pt(100) on the $c(2 \times 2)$ alloy and 5% of that on Pt(100) on the $3\sqrt{2}$ alloy surface. We cannot guarantee that these small amounts of D_2 do not originate from Pt-rich defect sites. Only a small amount of carbon was found in AES following TPD, which is fully consistent with these results.

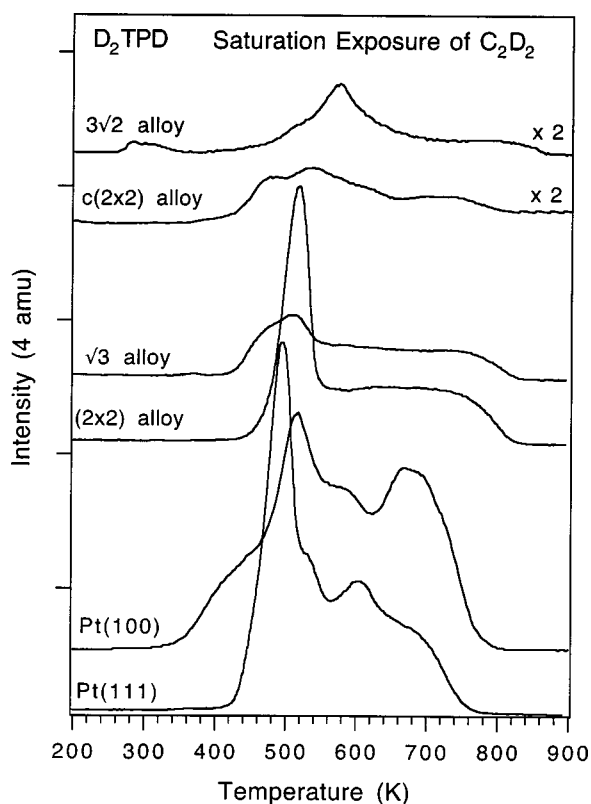


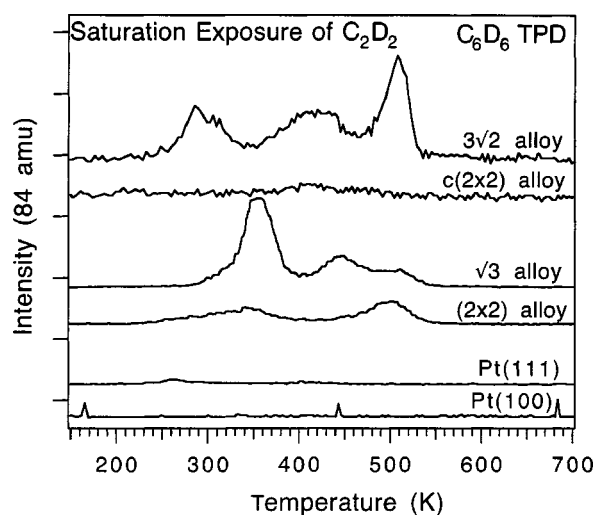
Figure 2. D_2 evolution in TPD after saturation exposure of d_2 -acetylene on Pt and Pt–Sn alloys at 100 K.

It is notable that the temperature for complete dehydrogenation of the carbonaceous residue formed from acetylene decomposition (polymerization) is increased by up to 100 K, from 760–780 K on the Sn-free Pt surfaces to 860 K on the $3\sqrt{2}$ -Sn/Pt(100) alloy.

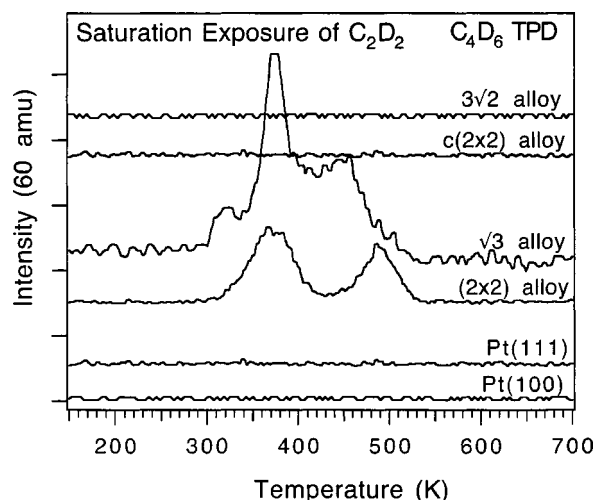
TPD curves for benzene desorption resulting from a saturation dose of acetylene on these surfaces are shown in figure 3(a). No benzene was desorbed on Pt(111) or Pt(100) surfaces. Acetylene is strongly rehybridized on clean Pt surfaces and, under UHV conditions, the only reaction pathway is decomposition to carbon and H_2 [11–16]. However, benzene desorption is observed following acetylene adsorption on both Sn/Pt(111) surfaces, and about 10% of the adsorbed acetylene monolayer was converted to benzene on the $\sqrt{3}$ alloy. Alloyed Sn weakens Pt– C_2D_2 bonding, decreases C_2D_2 rehybridization, and inhibits C_2D_2 decomposition. This ultimately leads to C–C bond coupling to give C_4 and C_6 surface species [18].

If the only factor involved in benzene formation was weaker chemisorption, then one would expect a higher amount of benzene formation on the $c(2 \times 2)$ -Sn/Pt(100) alloy than that on the (2×2) -Sn/Pt(111) alloy. However, no benzene signal was detected in TPD from the C_2D_2 monolayer on the $c(2 \times 2)$ -Sn/Pt(100) alloy. Obviously, some other factor (such as surface geometry) plays an important role in benzene formation and desorption.

On the $c(2 \times 2)$ -Sn/Pt(100) surface alloy, only a single-Pt atom ensemble exists (each Pt atom has only Sn nearest



(a)



(b)

Figure 3. (a) C_6D_6 (d_6 -benzene) and (b) C_4D_6 TPD traces after saturation exposures of d_2 -acetylene on these surfaces at 100 K.

neighbors). Hence, isolated Pt atoms with C_{4v} symmetry do not have acetylene cyclization activity under these conditions and apparently an ensemble of at least two Pt atoms is required for cyclotrimerization. However, given the low cyclotrimerization activity of Pd(100) [20], it could be that a surface with C_{4v} symmetry may not be favorable for this reaction and isolated Pt atoms with another surface symmetry may be active. For example, about 15% of the adsorbed acetylene monolayer undergoes cyclization and desorbs as benzene [23] on the $3\sqrt{2}$ alloy with $\theta_{Sn} = 0.67$. This amount was estimated from the XPS C(1s) intensity and benzene TPD peak areas. This implies that sites are present on this alloy in which Pt atoms are exposed at the surface in an ensemble which has locally C_3 or C_6 symmetry, perhaps with facets like the Sn/Pt(111) surface alloys. Support for this conjecture comes from a related study of CO on the two Sn/Pt(100) alloys, in which it was observed that the $3\sqrt{2}$ alloy showed more “Pt-like” chemistry than the $c(2 \times 2)$ alloy [25].

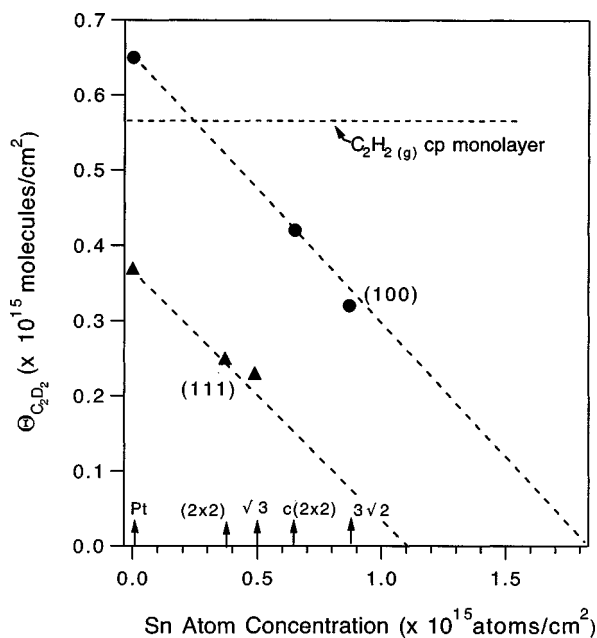


Figure 4. Comparison of acetylene monolayer coverage at 100 K.

On the Sn/Pt(111) alloys, a C_4 product desorbed as shown in figure 3(b). A mechanism has been proposed for benzene formation on Pd(111) that involves a C_4 -metallo-pentacycle intermediate [18]. The gas evolved in TPD is presumably butadiene that results from hydrogenation of a C_4 intermediate, but we cannot rule out a cyclobutene product from our limited data. This is an interesting contrast to the results for the two Sn/Pt(100) alloys, where we monitored all possible C_2 , C_4 and C_6 products but detected no butadiene or any other hydrocarbons desorbing during TPD. The addition of a third acetylene molecule to the C_4 intermediates must be strongly favored over hydrogenation of the C_4 intermediate on the $3\sqrt{2}$ -Sn/Pt(100) alloy compared to that on the Sn/Pt(111) alloy surfaces. This result probably arises simply from a lack of surface deuterium because of the reduced dehydrogenation activity on the $3\sqrt{2}$ -Sn/Pt(100) alloy.

Figure 4 provides a comparison of saturation coverages of acetylene in the chemisorbed monolayer on these surfaces at 100 K. On Pt(111), the saturation coverage of acetylene has been reported to be 0.25 ML (3.8×10^{14} molecules/cm²) at 100 K [18,26]. On this basis, the saturation C_2H_2 coverage decreases to 0.17 ML on the (2×2) alloy and 0.16 ML on the $\sqrt{3}$ alloy at 100 K [18]. On Pt(100), the acetylene monolayer coverage has been reported to be 0.5 ML (6.5×10^{14} molecules/cm²) at 100 K [11,12,23]. Using these references, the monolayer coverage decreases to 0.32 ML on the $c(2 \times 2)$ alloy and 0.25 ML on the $3\sqrt{2}$ alloy at 100 K. The monolayer coverage is unexpectedly different on these two Pt surfaces, and so it is not surprising that there is some controversy over the monolayer coverage of acetylene on clean Pt(111) [18,26–28]. This has been proposed to be either 0.25 ML [18,26] or 0.5 ML [27,28]. In figure 4 we have also indicated the saturation monolayer coverage calculated from

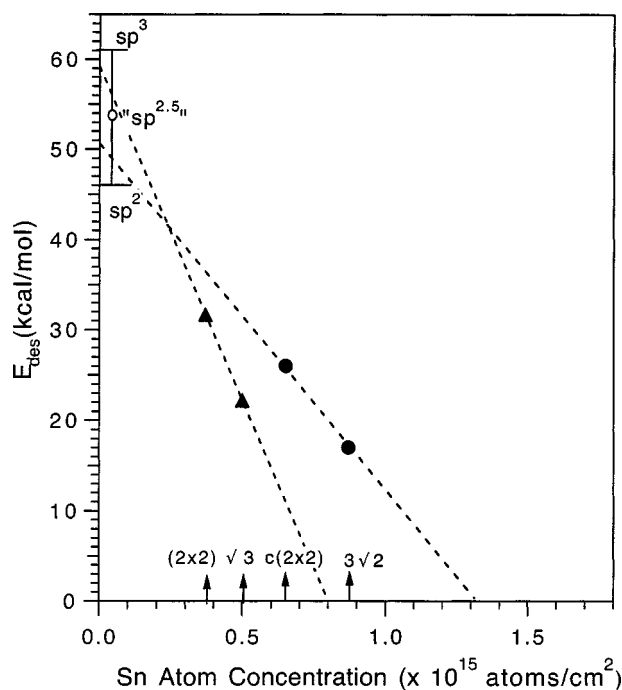


Figure 5. Influence of alloyed Sn on the acetylene desorption activation energy of the most strongly chemisorbed state, which is essentially the adsorption energy of the most strongly bound chemisorbed state on each of the four ordered Pt-Sn alloys. Values given by the brackets for clean Pt(100) and Pt(111) surfaces from predictions made in [29].

a closest packing model (θ_{cp}) with van der Waals contacts using the C_2D_2 gas phase structure. This coverage, $\theta_{cp} = 5.7 \times 10^{14}$ molecules/cm² (0.44 ML on Pt(100) and 0.37 ML on Pt(111)), sets a reasonable upper limit for the number of molecules in the chemisorbed layer. The coverage on Pt(100) has been reported to be slightly higher than θ_{cp} which can be explained by uncertainty in the experimental determination or perhaps by the fact that we used gaseous C_2H_2 molecular structure for calculation of θ_{cp} and formation of either sp^3 or sp^2 hybridized species upon chemisorption can lead to slightly higher coverages. The C_2H_2 monolayer coverage decreases 20–25% upon alloying 0.25–0.33 ML Sn into the Pt(111) surface. There is a larger decrease of 40–60% upon alloying 0.50–0.67 ML Sn into the Pt(100) surface. Such changes in the coverage of adsorbate due to site-blocking by surface modifiers is often modeled by using a Langmuirian adsorption type expression. This expression can be written as $\Theta_{C_2D_2} = (1 - a\Theta_{Sn})^b$, where a is the number of adsorption sites that are blocked by one modifier atom and b is the number of adsorption sites required for adsorption. For $b = 1$, both of the dashed lines in figure 4 give the same value of $a = 0.35$ for Sn/Pt alloy surfaces.

Figure 5 plots the desorption activation energy of acetylene on these surfaces, calculated using Redhead analysis. Because adsorption is not appreciably activated these energies correspond to adsorption energies. The adsorption energy of acetylene on clean Pt(111) and Pt(100) surfaces can be estimated by extrapolating the adsorption energy curves to zero Sn concentration. We note that these val-

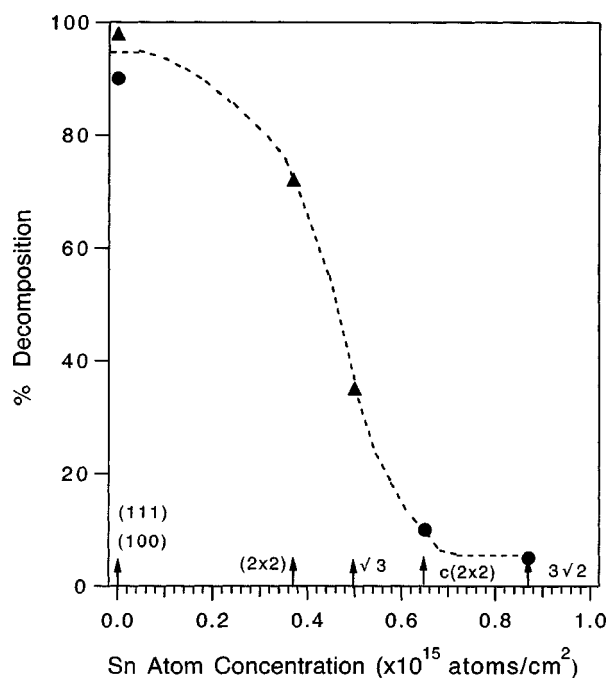


Figure 6. Fractional decomposition of acetylene in the monolayer (normalized to the saturation monolayer coverage on each surface) on the four Sn/Pt(111) and Sn/Pt(100) surface alloys.

ues for acetylene adsorption energy on (111) and (100) Pt surfaces agrees well with the “ $sp^{2.5}$ ” adsorption energy of 54 kcal/mol predicted from sp^3 (61 kcal/mol) and sp^2 (46 kcal/mol) C_2 species as estimated using the QVB theory by Koel and Carter [29] and a Pt–C covalent σ -bond strength of $D(\text{Pt–C}) = 53$ kcal/mol. Alloyed Sn weakened the chemisorption bond strength of acetylene by 45–65% on these surfaces and the acetylene desorption activation energy decreases concomitantly with increasing surface Sn concentration. However, the C_2D_2 –Pt bond strength on $c(2 \times 2)$ alloy on Pt(100) with $\theta_{\text{Sn}} = 0.5$ ML is apparently higher than that on the (2×2) alloy on Pt(111) with $\theta_{\text{Sn}} = 0.33$ ML.

The amount of acetylene decomposition (after normalizing to the saturation monolayer coverage) on each of the surfaces studied is shown in figure 6. On the Sn/Pt(111) alloys, 72 and 35% of the acetylene monolayer decomposed for $\theta_{\text{Sn}} = 0.25$ and 0.33, respectively, in the Pt(111) surface. On the Sn/Pt(100) alloys, acetylene adsorption is largely reversible and 90% of the acetylene monolayer reversibly desorbed on the $c(2 \times 2)$ alloy. On the (2×2) -Sn/Pt(111) alloy, three-fold pure Pt sites are present but there are no two adjacent three-fold pure Pt sites. Only two-fold bridge and atop sites are present on the $\sqrt{3}$ alloy, with all of the pure Pt three-fold sites eliminated, but still about 35% of acetylene monolayer decomposed on this surface. On the $c(2 \times 2)$ alloy, each surface atom of Pt is isolated, i.e., there are no Pt–Pt nearest neighbors, and a “checker board” pattern of Pt and Sn is formed. The strong suppression of decomposition of acetylene on both Sn/Pt(100) alloys can be attributed to an ensemble requirement of at least a pure

Pt two-fold bridge site to stabilize the transition state or reaction products of acetylene decomposition.

4. Conclusion

C_2H_2 is a reactive molecule with a low H:C stoichiometry used to model coking reactions on Pt and Pt–Sn alloy surfaces. Sn reduced the C_2H_2 chemisorption bond strength and reactivity for dissociative adsorption of C_2H_2 compared to Sn-free Pt surfaces. Also, the temperature for complete dehydrogenation of the carbonaceous residue formed from C_2H_2 decomposition was increased by up to 100 K. Gaseous C_4 and C_6 products were formed from C–C bond coupling reactions of chemisorbed C_2H_2 in UHV. Acetylene chemisorption on these Sn/Pt alloyed surfaces is relatively structure-insensitive, but acetylene reaction and decomposition is structure-sensitive. Our results indicate that a single Pt atom is sufficient to chemisorb acetylene, but an ensemble of at least two Pt atoms is required for decomposition activity. C_2D_2 cyclotrimerization reactions on the $3\sqrt{2}$ alloy surface indicate that reconstruction to produce this alloy leads to the formation of Pt sites that have a local C_3 symmetry.

Acknowledgement

This work was supported by the US Department of Energy, Office of Basic Energy Sciences, Chemical Sciences Division.

References

- [1] E. Marlen, P. Beccat, J.C. Bertolini, P. Delichere, N. Zanier and B. Didillon, *J. Catal.* 159 (1996) 178.
- [2] Y. Zhou and S.M. Davis, *Catal. Lett.* 15 (1992) 51.
- [3] Y.X. Li, K.J. Klabunde and B.H. Davis, *J. Catal.* 128 (1991) 1.
- [4] G. Meitzner, G.H. Via, F.W. Lytle, S.C. Fung and J.H. Sinfelt, *J. Phys. Chem.* 92 (1988) 2925.
- [5] R. Srinivasan, L.A. Rice and B.H. Davis, *J. Catal.* 129 (1991) 257.
- [6] H. Lieske and J. Volter, *J. Catal.* 90 (1984) 96.
- [7] R. Srinivasan, R.J. De Angelis and B.H. Davis, *J. Catal.* 106 (1987) 449.
- [8] K. Balakrishnan and J. Schwank, *J. Catal.* 132 (1991) 451.
- [9] R.D. Cortright and J.A. Dumesic, *J. Catal.* 148 (1994) 771.
- [10] R.D. Cortright and J.A. Dumesic, *J. Catal.* 157 (1995) 576.
- [11] T.E. Fischer, S.R. Kelemen and H.P. Bonzel, *Surf. Sci.* 64 (1977) 157.
- [12] T.E. Fischer and S.R. Kelemen, *J. Vac. Sci. Technol.* 15 (1978) 607.
- [13] H. Ibach and S. Lehwald, *J. Vac. Sci. Technol.* 15 (1978) 407.
- [14] L.L. Kesmodel, L.H. Dubois and G.A. Somorjai, *J. Chem. Phys.* 70 (1979) 2180.
- [15] M. Salmeron and G.A. Somorjai, *J. Phys. Chem.* 86 (1982) 341.
- [16] C.E. Megiris, P. Berlowitz, J.B. Butt and J.J. Kung, *Surf. Sci.* 159 (1985) 184.
- [17] N.A. Avery, *Langmuir* 4 (1988) 445.
- [18] C. Xu, J.W. Peck and B.E. Koel, *J. Am. Chem. Soc.* 115 (1993) 751.
- [19] M.T. Paffett and R.G. Windham, *Surf. Sci.* 208 (1989) 34.
- [20] S.H. Overbury, D.R. Mullins, M.T. Paffett and B.E. Koel, *Surf. Sci.* 254 (1991) 45.

- [21] M.T. Paffett, A.D. Logan, R.J. Simonson and B.E. Koel, *Surf. Sci.* 250 (1991) 123.
- [22] Y. Li and B.E. Koel, *Surf. Sci.* 330 (1995) 193.
- [23] C. Panja, N.A. Saliba and B.E. Koel, in preparation.
- [24] R.G. Windham, M.T. Bartram and B.E. Koel, *J. Phys. Chem.* 92 (1988) 2862.
- [25] C. Panja and B.E. Koel, *Isr. J. Chem.* 38 (1998) 365.
- [26] M. Abon, J. Billy and J.C. Bertolini, *Surf. Sci.* 171 (1986) L387.
- [27] N. Freyer, G. Pirug and H.P. Bonzel, *Surf. Sci.* 125 (1983) 327.
- [28] N. Freyer, G. Pirug and H.P. Bonzel, *Surf. Sci.* 126 (1983) 487.
- [29] B.E. Koel and E.A. Carter, *Surf. Sci.* 226 (1990) 339.